



4-3-11

MITIGATION OF LIQUEFACTION POTENTIAL

Edward E. RINNE,¹ Craig S. SHIELDS,²
and Christopher R. NARDI³

¹Kleinfelder, Walnut Creek, California

²Harding Lawson Associates, San Francisco, California

³The Mark Group, Pleasant Hill, California

SUMMARY

A large, low-rise apartment complex, built over potentially liquefiable soils adjacent to San Francisco Bay illustrates current California practice for investigating the liquefaction potential and design/construction techniques to reduce its effects. Lateral spreading effects were mitigated by constructing a stone column buttress adjacent to the shoreline. Post-tensioned concrete slabs were used to increase rigidity beneath the structures to reduce liquefaction-induced settlement effects.

INTRODUCTION

Seismic liquefaction potential and the effects on existing and proposed construction projects and its subsequent mitigation have become common geotechnical design considerations in seismically active areas of the world. Tailoring both effective and economically feasible mitigation measures for residential, commercial, and other light to moderately loaded construction without compromising safety is particularly challenging, considering the narrow range of feasible unit-area development costs.

A 42-unit wood-frame apartment complex consisting of 2 and 3 stories built over potentially liquefiable soils adjacent to San Francisco Bay is a case in point.

SITE CONDITIONS

The site was a tidal marsh on the northeast shore of the San Francisco Bay and was reclaimed by hydraulic filling about 50 years ago. Formerly part of a shipyard, the site is being redeveloped for residential and water recreational uses.

The San Francisco Bay Area is both geologically and seismically active. The site rests upon unconsolidated deposits of artificial fill, Holocene bay deposits, and alluvium. The artificial fill is composed of angular sand, gravel, and construction debris overlying hydraulically placed sand, silt, and clay. Holocene bay deposits consist of interbedded fine sand, silt, and clay. Alluvial deposits beneath the bay mud deposits consist of mixed, dense sands and stiff clays. Published maps of the area indicate an alluvium thickness approximately 150 to 200 feet (45 to 60m) with Cretaceous rocks of the Franciscan Formation at depth.

The San Andreas Fault system dominates seismic activity in the San Francisco Bay Area, as shown in Fig. 1. Near the site, the Hayward Fault, capable of generating M7.5 events, is approximately 4.5 kilometers to the northeast with the San Andreas Fault (M8.25) approximately 25 kilometers to the southwest.

Ground motion parameters for liquefaction evaluations were assessed using the basic approach by Cornell (Ref. 1) utilizing historical seismicity data assigned 80 percent to surrounding faults, with the remainder randomly distributed as an area source. The design-level earthquake was defined as an earthquake occurring at the site with a 50-percent chance of exceedance in a 50-year design life. The analysis indicated that the design earthquake was one with a magnitude of 6.5, developing a peak ground acceleration of 0.3g. An earthquake having a 10-percent chance of exceedance in 50 years was analyzed similarly as developing a peak ground acceleration of 0.45g.

Subsurface conditions along and behind the shoreline were evaluated using standard penetration test (SPT) borings and cone penetration test (CPT) probes. Twenty-four SPT borings and 12 CPT probes were advanced prior to mitigation construction. After construction, 10 borings and 12 CPT probes were advanced. The depths of the soil borings ranged between 6 and 21.5 meters. CPT probes ranged between 6.5 and 13.6 meters. Borings were advanced using solid stem auger, hollow stem auger, and rotary mud techniques. Significantly lower N values were recorded in the auger borings, and analyses were subsequently based on N values from rotary mud borings.

A typical profile is shown in Fig. 2. Hydraulic fill and bay deposits extend to approximately elevation -11 (-3.4 meters), National Geodetic Vertical Datum, where they are underlain by stiff and dense alluvial soils. The fill and bay deposits at the site are predominately nonplastic sandy silts and silty sand with some layers of cohesive soils. SPT N values of 2 to 15 and CPT q_c values of 10 to 70 kilograms per square centimeter were typically recorded in these soils. Typical grain size distributions in these soils are shown in Fig. 3. Fines content (percent passing #200 sieve) varies between 10 and 93 percent and averages 45 percent. Measured clay content (less than 0.002mm) varies between 4 and 10 percent. However, all silt and sand samples were nonplastic.

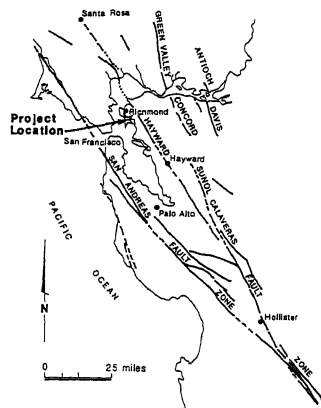


FIGURE 1. Project Location and Fault Map

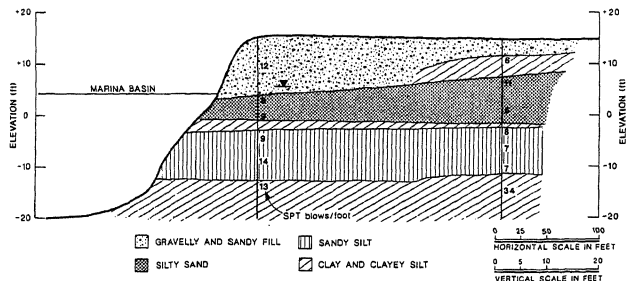


FIGURE 2. Typical Soil Profile

ANALYSES

The liquefaction potential of the loose to medium dense silty sands and sandy silts was evaluated using the analytical-empirical procedure based on the liquefaction behavior of saturated clean and silty sands during historic earthquakes by Seed, et al. (Ref. 2). The primary data used in the evaluation consisted of SPT N values. N values from field investigations were corrected for overburden pressure, hammer type, drill rod length, and type of sampling tube. Also, the N values were increased to account for fines content as proposed by Seed (Ref. 3). The resulting $(N_1)_{60}$ values varied between 11 and 22 with an average value of 15.

Using the peak ground acceleration for the design earthquake, the cyclic shear stress ratio was computed for several depths using the procedure outlined by Seed and Idriss (Ref. 4). The computation indicated that the cyclic shear stress ratio for the design earthquake averages approximately 0.25 in liquefiable deposits.

The liquefaction analyses indicated that continuous deposit of sands and silts would likely liquefy during the design earthquake. Furthermore, as shown in Fig. 4, the predicted shear strain potential of silts and sands following liquefaction is large (approximately 20 percent). Because the liquefiable deposit is adjacent to the bay and lateral spreading during an earthquake is a strong possibility, there was a significant risk to inland development.

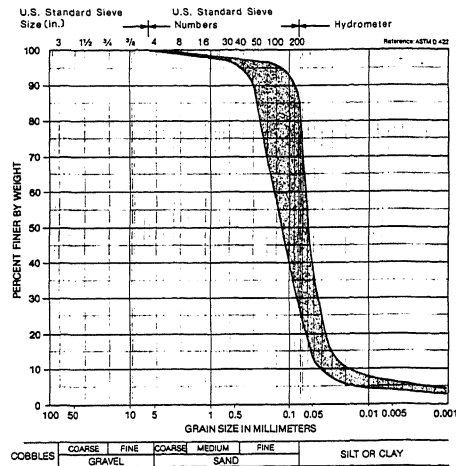


FIGURE 3. Grain Size Distribution

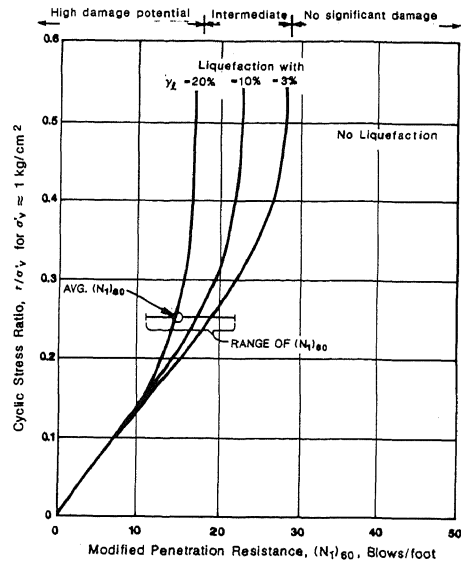


FIGURE 4. Liquefaction Susceptibility and Shear Strain Potential Chart with SPT Data (M=6.5 Earthquake)

The developer and city officials decided that eliminating the liquefaction potential over the full extent of the continuous liquefiable deposit would be uneconomical. Therefore, a "buttress" was installed at the shoreline boundary through the liquefiable deposit to resist potential lateral spreading during an earthquake.

Liquefaction-induced settlements were estimated using the proposed relationship between cyclic stress ratio and volumetric strain for clean sands by Tokimatsu and Seed (Ref. 5). Using this relationship with an average $(N_1)_{60}$ value of 15 and an average cyclic stress ratio of 0.25, a volumetric strain of 2 percent was obtained. Based on an average 12-foot thickness of liquefiable material, a corresponding settlement of 2 to 3 inches (50 to 75mm) was calculated. For this site, the settlement due to fill and structural loads was also estimated to be about 3 inches (75mm).

Liquefaction of underlying soils would probably be incomplete because of clay stringers. Project building grades, approximately 10 feet (3m) above liquefiable soils, should significantly reduce the risk of ground rupture based on case histories in Ref. 6. Because of this, and the presence of significant fines content, actual seismic settlement would probably be less than the calculated values.

DESIGN OF MITIGATION MEASURES

Several mitigation alternatives were considered in developing a buttress that would be stable and buildable under the economic and time constraints of the project. Because of the high fines content of the liquefiable deposit (an average of 45 percent), it was believed that ground modification methods, such as deep dynamic compaction and vibro-floatation (vibro-compaction), would not densify the liquefiable deposit adequately to form an effective buttress. Consequently, it was decided to construct the buttress using vibro-replacement stone column techniques.

The buttress consists of 42-inch diameter (1.07m) stone columns placed 6 feet (1.8m) on center in a square grid extending about 1 foot (0.3m) below the bottom of the liquefiable zone at elevation -11 feet, as shown in Fig. 5. The buttress is trapezoidal in cross section with a crest and base width of about 16 and 58 feet (5 to 18m), respectively. It extends along the shoreline approximately 1,000 feet (300m). The inland face of the buttress slopes at about 1:1 and the outboard (bay side) face slopes at about 2:1 (horizontal to vertical). The crest is at elevation +6 feet (+1.8m).

The stone column buttress is expected to limit lateral spreading in two ways. First, the columns, which consist of dense, liquefaction-resistant crushed rock, reinforce the slope along the shoreline. Second, the installation of the columns increases the resistance to liquefaction of sands and silts between the columns by densification, thereby providing increased lateral confinement and a drainage path to dissipate earthquake-induced pore pressures. The stability of the buttress slope was checked for an assumed loss of shear strength of saturated soils behind the buttress.

Mitigation measures for liquefaction-induced settlement consisted of providing a relatively rigid foundation utilizing a post-tensioned concrete slab tied into continuous perimeter footings. The slab is 8 inches (200mm) thick with 1/2-inch (12mm) tendons at 3 feet (0.9m) spacing each way in the center of the slab. Similar systems have been successfully used throughout California at sites where significant ground movement is expected due to consolidation or expansive soils.

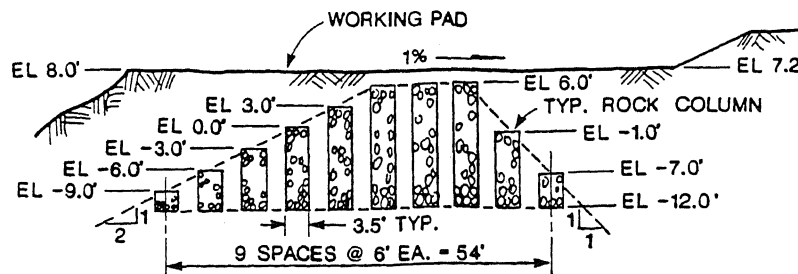


FIGURE 5. Typical Buttress Cross Section

CONSTRUCTION

The stone column buttress was constructed by G.K.N. Hayward Baker, Inc. The stone columns were constructed using two 1-1/2-foot diameter, 12-foot long downhole vibrators suspended from cranes. The vibrators were advanced into the ground dry primarily by their vibratory energy. When the tip of the vibrator reached elevation -12 feet, the hole created by the vibrator was backfilled using a bottom-feed system with 3/8-inch by 1-inch crushed rock. The rock was placed in about 3-foot thick lifts. For each lift, the probe was raised and lowered several times to feed the desired amount of crushed rock, push the rock laterally, and vibrate it into a dense 42-inch diameter column. This procedure continued until the design height of the column was reached.

PERFORMANCE TESTING

To determine the effect of placing stone columns on liquefiable deposits, 10 test borings were drilled and 12 CPT probes were advanced between the stone columns. CPT tip-resistance values were modified for overburden pressures using correction factors proposed by Robertson and Campanella (Ref. 7). Average pre- and post-construction modified CPT tip-resistance (q_{c1}) values are shown in Fig. 6. The correlations between liquefaction resistance and q_{c1} values proposed by Robertson and Campanella (Ref. 7) and Seed, et al. (Ref. 8) were used to evaluate the liquefaction susceptibility of the sand and silt deposits. As shown on Fig. 6, the liquefaction potential of the deposits prior to installing the stone columns was moderate to high using the Seed correlation, and high using the Robertson and Campanella correlation. The average q_{c1} value increased by approximately 45 kg/cm² following column installation. Using the CPT correlations, the post-construction liquefaction potential of the deposits was considered to be low for the design earthquake. It should be noted that increases in CPT tip resistance were significantly higher in deposits with lower silt contents.

Average pre- and post-construction $(N_1)_{60}$ values are plotted in Fig. 7. Fig. 7 presents the correlation between liquefaction resistance and $(N_1)_{60}$ values for the maximum credible earthquake (M7.5). As shown, the average $(N_1)_{60}$ value increased averaging 7 blows/foot. Despite the increase, the liquefaction potential of the soils remained high. However, the estimated shear strain potential of the liquefied deposits decreased from greater than 20 percent to approximately 10 percent. Consequently, some lateral spreading could occur along the shoreline during a maximum credible earthquake. Although a liquefaction-induced flow-type failure is not expected, slope deformation and lateral spreading during the design earthquake are expected to be small.

CONCLUSIONS

Liquefaction-prone sites can be safely and economically developed for light to moderate construction using various techniques including limited ground improvement and stiffened foundations. The vibro-replacement stone column technique was moderately effective in densifying very silty site soils, increasing the SPT and CPT resistance of these soils by approximately 45 percent. This increased resistance should provide a measure of safety for liquefaction-induced ground movements consistent with design procedures for structural components designed in accordance with current Uniform Building Code procedures.

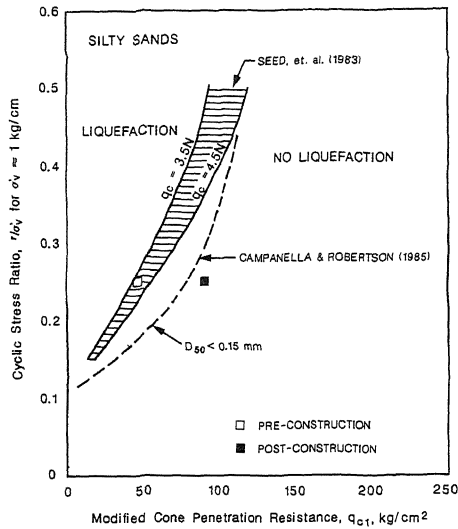


FIGURE 6. Comparison of Pre-Construction and Post-Construction CPT Data (M=6.5 Earthquake)

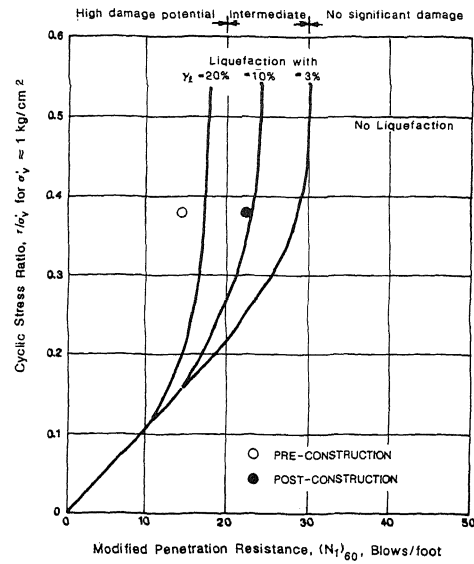


FIGURE 7. Comparison of Pre-Construction and Post-Construction SPT Data (M=7.5 Earthquake)

REFERENCES

1. Cornell, C.A., "Engineering Seismic Risk Analyses," Seismological Society of America Bulletin, V. 58, No. 5, pp. 1583-1606 (1968).
2. Seed, H.B., Tokimatsu, K., and Harder, L.F., "The Influence of SPT Procedures in Soil Liquefaction Resistance Evaluations," Report UCB/EERC-84/15, University of California, Berkeley (October 1984).
3. Seed, H.B., "Design Problems in Soil Liquefaction," J. Geotech Engineering, ASCE, 113 (8), pp. 827-845 (1987).
4. Seed, H.B., and Idriss, I.M., "A Simplified Procedure for Evaluating Soil Liquefaction Potential," J. Soil Mech Found. Div, ASCE, 97 (9), pp. 1249-1274 (1971).
5. Seed, H.B., and Tokimatsu, K., "Evaluation of Settlement in Sands Due to Earthquake Shaking," J. Geotech Engineering, ASCE, 113 (8), pp. 861-878 (1987).
6. Ishihara, K., "Stability of Natural Deposits During Earthquakes," Proc. 11th ICSMFE, V. 1 (1985).
7. Robertson, P.K. and Campanella, R.G., "Liquefaction Potential of Sands Using the CPT," J. Geotech Engineering, ASCE, 111 (3), pp. 384-403 (1985).
8. Seed, H.B., Idriss, I.M., and Arango, I., "Evaluation of Liquefaction Potential Using Field Performance Data," J. Geotech Engineering, ASCE, 109 (3), pp. 458-482 (1983).